APPLIED ORGANOMETALLIC CHEMISTRY, VOL. 10, 83–99 (1996)

Si/C Phases from the IR Laser-induced Decomposition of Silacyclobutane and 1,3-Disilacyclobutane

Z. Bastl,* H. Bürger,†‡ R. Fajgar,§ D. Pokorná,§ J. Pola,‡§ M. Senzlober,† J. Šubrt¶ and M. Urbanová§

* J. Heyrovský Institute of Physical Chemistry 182 23, Prague 8, Czech Republic, † Anorganische Chemie, FB 9, Universität-GH, W-5600 Wuppertal 1, Germany, § Institute of Chemical Process Fundamentals, Rozvojova str 135, 165 02 Prague 6, Czech Republic, and ¶ Institute of Inorganic Chemistry, 25 068 Řež, near Prague, Czech Republic

CO_2 laser-induced infrared multiphoton decomposition (IRMPD) and SF_6 photosensitized decomposition (LPD) of silacyclobutane (SCB) and 1,3-disilacyclobutane (DSCB) in the gas phase results in the very efficient deposition of Si/C/H and SiC materials, and it is inferred that the process is dominated by formation of transient silene; silene rearrangement to methylsilylene; silene and methylsilylene dehydrogenation; and polymerization of $SiCH_n$ ($n < 4$) species. The deposits are sensitive to oxygen.

Decomposition and SiC formation are favoured with IRMPD experiments conducted with high-energy fluxes. The laser technique is promising for low-temperature chemical vapour deposition of amorphous SiC.

Keywords: laser; chemical vapour deposition; thin films; Si/C/H materials; silacyclobutane; 1,3-disilacyclobutane; silicon carbide

INTRODUCTION

Chemical vapour deposition (CVD) induced by heat, plasma or photolysis is an approved technique for the production of SiC and Si/C/H materials which find use as advanced ceramics or in electronic applications. In pursuit of alternative volatile precursors to SiC and Si/C/H, various specially designed hydridocarbosilanes offering improved control of the Si/C stoichiometry and lower deposition temperatures have been tested (see for example Refs. 1–11).

Of these potential precursors, those which are sources of silene ($H_2Si{=}CH_2$) or its partner in thermal equilibrium, methylsilylene [$CH_3(H)Si$:] (see for example Refs. 12–16) seem most promising due to a built-in 1 : 1 Si/C ratio, to relatively weak Si–H bonds and, most of all, to a strong double bond between silicon and carbon. While methylsilylene can be produced by photolysis[17,18] or thermolysis[16,19,20] of methylsilane, convenient preparation routes for silene could be the thermolysis of silacyclobutane (SCB), silabicyclo[2.2.2]octadienes (SBCOD), and 1,3-disilacyclobutane (DSCB). SCB and DSCB experience significant strain in the four-membered ring and offer the prospect of lower deposition temperatures. However, thermal decompositions of these compounds (SCB,[13,21–23], SBCOD[14,24,25] and DSCB[26]) were studied under conditions where heterogeneous steps taking place at hot surfaces can complicate clean decomposition by enhancing secondary reactions; it was observed that both SCB and DSCB decompositions are rather complex.

We thought that an entirely homogeneous mechanism procured in thermal IR laser-induced decompositions[27–29] may be dominated by a clean decomposition into primary silene (Scheme 1), which can undergo either dehydrogenation or polymeriztion/dehydrogenation to yield the desired Si/C/H and/or Si/C materials (Scheme 2).

The possibly minor rearrangement of silene into methylsilylene might also be followed by a dehydrogenation or polymerization/dehydrogenation and yield the same products (Scheme 2).

We assumed that direct gas-phase dehydrogenation of the H_4SiC transients can be achieved due to an excess of the energy available from the exothermicity of the precursor cleavage and also due to the direct absorption of laser radiation in the short-lived H_4SiC species. If the gas-phase

‡ Author to whom correspondence should be addressed.

CCC 0268–2605/96/020083–17

Received 22 February 1995
Accepted 23 May 1995

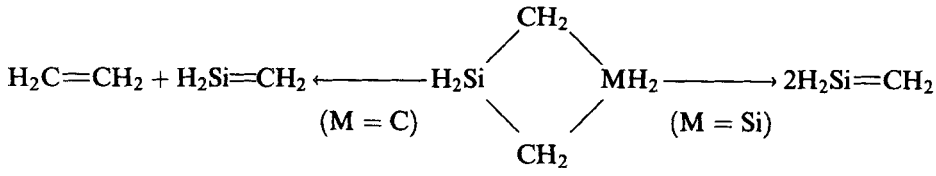

Scheme 1 Homogeneous decomposition of SCB or DSCB into primary silene.

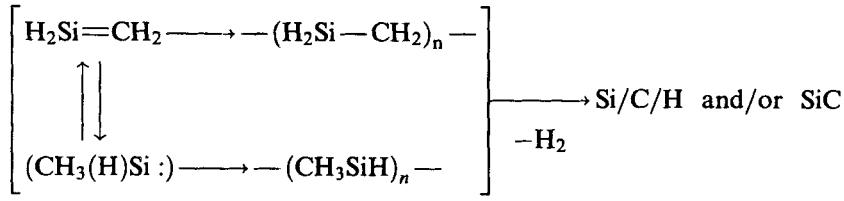

Scheme 2 Formation of Si/C/H and SiC materials from silene.

polymerizations were not accompanied by dehydrogenation, the deposited materials with relatively high hydrogen content might be dehydrogenated afterwards and yield SiC in a separate process.

There are several prerequisites for these assumptions:

(1) The silenes generated by IR laser-photosensitized decomposition (LPD) of silacyclobutanes $R_2\overline{SiCH_2CH_2CH_2}$ with R = H, $CH_2{=}CH$ and $HC{\equiv}C$ prefer polymerization,[30–32] although they cyclodimerize when generated from the silacyclobutanes by conventional (hot-wall) decomposition.[33,34]

(2) Linear polymethylsilane/polysilene (prepared until now solely in solution[35–38]) can give high yields of ceramic material upon proper thermal treatment,[38,39] since an initial step of this process is cross-linking by latent Si–H bonds.

(3) The IR spectrum of silene[25] is consistent with good absorption of the CO_2 laser radiation by this transient, which enables excitation of silene by the laser radiation once it is generated. This could result in silene dehydrogenation.

(4) At temperatures comparable with those effective during laser decompositions (600–1150 °C), $H_2Si{=}CH_2$ is far more stable than $CH_3(H)Si$:, and estimates of the forward and reverse reaction rates of the $CH_3(H)Si: \rightarrow H_2Si{=}CH_2$ equilibrium are much in favour of silene formation.[15,16]

To our knowledge, there are only two reports on CVD of SiC from SCB[16] and DSCB,[40] both processes having been studied only under conditions of hot substrates facilitating heterogeneous steps.

In this paper we present an examination of the laser-driven decomposition of SCB and DSCB carried out via direct excitation of all the compounds by pulsed CO_2 laser radiation (infrared multiphoton decomposition, IRMPD), and also an examination of the continuous-wave CO_2 laser sulphur hexafluoride (SF_6)-photosensitized decomposition (LPD) of SCB and DSCB. We give attention to the progress of these decompositions and to the properties of the deposited materials.

EXPERIMENTAL

High-resolution gas-phase FTIR spectra were recorded with a Bruker 120 HR interferometer operating at a resolution (MOPD) of $3.4 \times 10^{-3}\,cm^{-1}$ and $2.2 \times 10^{-3}\,cm^{-1}$ for SCB and DSCB, respectively. A KBr beam splitter, globar source and MCT 800 detector were employed and trapezoidal apodization applied. The spectra were calibrated with lines of residual H_2O in the interferometer.[41] Wavenumber precision is better than $1 \times 10^{-3}\,cm^{-1}$.

The IRMPD experiments were performed using a grating-tuned transversely excited atmospheric

(TEA) CO_2 laser (P. Hilendarski Plovdiv University, 1300 M model) operated on the P(14), P(20) and P(28) (SCB) and R(18), R(20) and R(26) (DSCB) lines of the 00 °1→10 °0 transition (949.48, 944.19, 936.80, 974.62, 975.93 and 979.71 cm^{-1}, respectively). These wavelengths were confirmed by using a model 16-A spectrum analyser (Optical Engineering Co.). The incident laser beam was rectangular (1.8 and 1.0 cm per side, or *ca* 0.6 and 0.3 cm per side when focused), and a typical temporal profile of the pulse, as measured with a Rofin photon drag detector, consisted of a 150 ns FWHM (full width at half-maximum) peak followed by a tail of approximately 1 μs. Focusing of the laser beam was achieved using a NaCl lens (focal length 8 cm) located just before the entrance window of the reactor. The laser energy was measured with a laser energy pyroceramic sensor (Charles University m1-1JU model).

The LPD experiments were carried out in a simple reaction cell using a CW CO_2 laser which was operated at the P(20) line of the 00 °1→10 °0 transition (944.19 cm^{-1}), and had its beam focused by a germanium (Ge) lens to achieve an incident irradiation energy of 30 W cm^{-2}.

The energy absorbed in SCB and DSCB was determined by measuring the difference in energy transmitted by the cell when filled with gases and when empty.

Some LPD experiments were also performed in a previously described apparatus[41] in which the irradiated cell was coupled via a sampling valve with the gas chromatograph. The samples of equimolar amounts of the silacycle and SF_6, and of n-butane (internal standard, *ca* 50 mol% SF_6) and an excess of argon (diluent gas, total pressure 4 kPa) were prepared in a standard vacuum manifold and introduced to the reactor for the irradiation. The progress of the decomposition with the gaseous mixtures irradiated at measured intervals was monitored using the sample valve and the gas chromatograph.

Irradiation of gaseous SCB and DSCB (in the absence of SF_6 as sensitizer) was conducted in a cylindrical (3.6 cm i.d., 10 cm long) Pyrex cell which was furnished with NaCl or KBr windows and a PTFE stopcock used for filling and evacuating the vessel. Samples of SCB and DSCB, introduced into the cell using a standard vacuum-line, were irradiated with a number of pulses of different energy flux, or by continuous radiation, and changes in the composition of the cell contents were monitored by gas chromatography (gas chromatograph Shimadzu 14 A coupled with Chromatopac C-R5A computing integrator) and by FTIR (Nicolet, model Impact 400) and GC–MS (Shimadzu, model QP 1000 quadrupole spectrometer) methods. For chromatographic separation of the decomposition products, a programmed temperature (30–150 °C) and columns packed with Porapak P (1.3 m) as well as OV-1 sillicon elastomer (3 m) were used.

Reaction progress was estimated by using diagnostic bands at 1120 and 2950 cm^{-1} (SCB) and 642, 650 and 1365 cm^{-1} (DSCB).

Scavenging experiments for identifying intermediate species were carried out in a five-fold excess of buta-1,3-diene. Volatile products were analysed by GC–MS spectroscopy.

In order to evaluate the properties of the deposit by FTIR spectroscopy, scanning electron microscopy (SEM) techniques and X-ray photoelectron spectroscopy (ESCA or XPS) deposits were produced on different substrates (metal, NaCl) housed in the vessel before irradiation. FTIR spectra of the deposits on NaCl substrates or the NaCl windows of the reactor were taken after evacuation of the reactor. For XPS and SEM measurements the samples had to be transported from the reactor and exposed to ambient atmosphere.

XPS measurements were performed using a VG ESCA 3 Mk II electron spectrometer. The spectra were recorded with Al Kα radiation and an electrostatic hemispherical analyser operated in the fixed transmission mode. Detailed spectral scans were taken over the Si(2*p*), C(1*s*), O(1*s*) and Si($KL_{23}L_{23}$) regions. The sum of the kinetic energy of Si($K_{23}L_{23}$) Auger electrons and the binding energy of Si(2*p*) electrons, defined as the Auger parameter, was calculated from the measured data. This value is independent of the static charge referencing procedure and therefore is obtained with higher accuracy than the energy of either set of electrons alone. Quantification of the element concentration ratios was accomplished by correcting integral intensities of photoelectron peaks for their cross-sections[43] and accounting for the dependence of electron mean free paths on kinetic energy.[44] Curve fitting of overlapping spectra was carried out using lines of Gaussian–Lorenzian shape and a damped nonlinear least-squares technique.[45]

Scanning electron microscopy studies of the deposits were performed on an ultrahigh-vacuum instrument (Tesla BS 350).

Samples of SCB[46] and DSCB[47,48] were pre-

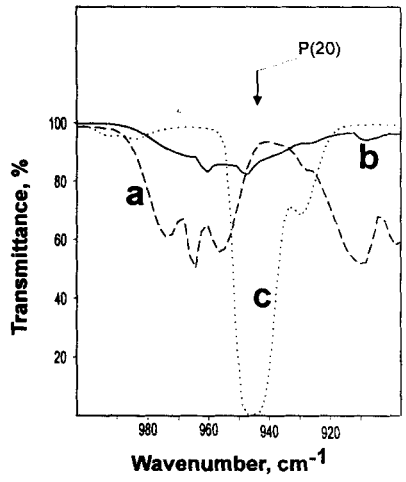

Figure 1 IR spectra of DSCB (**a**), SCB (**b**) and SF_6 (**c**) (all 0.3 kPa, 10 cm path) in the emission region of the CO_2 laser.

pared according to previously reported procedures, and their purity (better than 99%) was checked by gas chromatography.

RESULTS AND DISCUSSION

SCB and DSCB show strong absorptions in the emission range of the CO_2 laser (Fig. 1) and can be decomposed by tuning the TEA CO_2 laser radiation into their $\delta(SiH_2)$ absorption band. In order to evaluate coincidences of SCB and DSCB with available laser lines, high-resolution spectra (line width *ca* 3×10^{-3} cm^{-1} and 2×10^{-3} cm^{-1} for SCB and DSCB, respectively) were recorded. These are illustrated in Figs 2 and 3.

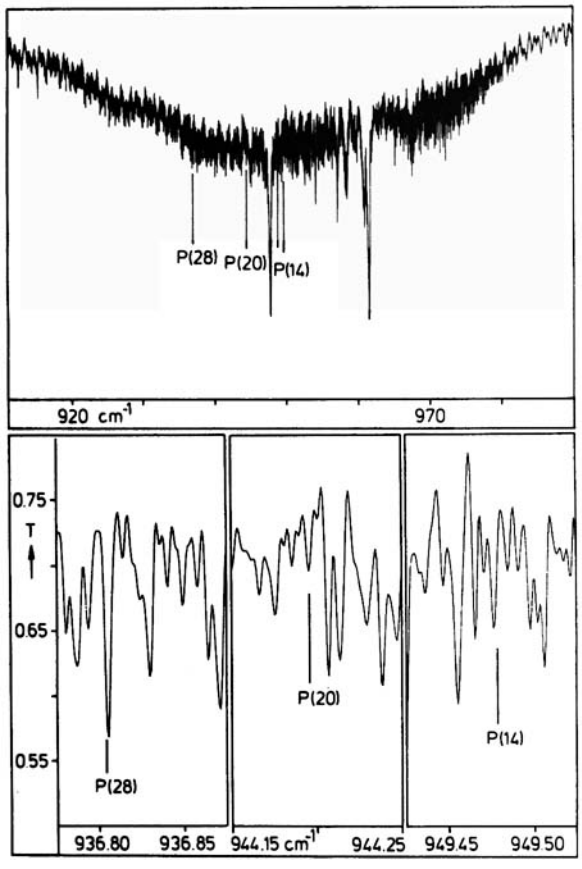

Figure 2 High-resolution IR spectra of SCB [*ca* 1 mbar, 28 cm cell, resolution (MOPD) 3.4×10^{-3} cm^{-1}]. Top, survey spectrum; bottom, details in the region of the 10P(28) and 10P(14) lines, with positions of the laser lines indicated.

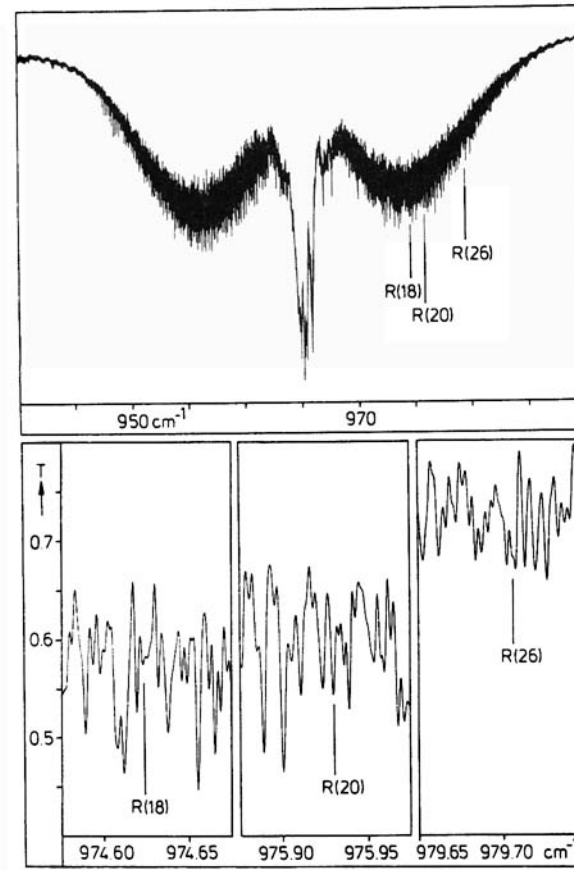

Figure 3 High-resolution IR spectrum of DSCB [*ca* 1 mbar, 28 cm cell, resolution (MOPD) 2.2×10^{-3} cm^{-1}]. Top, survey spectrum; bottom, details in the region of the 10R(18), 10R(20) and 10R(26) lines, with positions of the laser lines indicated.

Table 1 IRMPD of SCB

Run	Irradn line	Focused	Energy in pulse[a] (J)	No. of pulses	Pressure (kPa)	Decompn. progress (%)	Gaseous products (mol/mol of SCB decomposed)					
							CH_4	C_2H_4	C_2H_2	$CH_3CH : CH_2$	CH_3SiH_3	$n\text{-}C_3H_7SiH_3$
1	P(14)	No	0.60	1500	4	40	0.007	0.85	—	0.12	0.12	0.010
2	P(28)	No	1.0	2000	3	58	0.007	0.83		0.16	0.12	0.020
3	P(14)	Yes	0.90	35	4	42	0.004	0.60	0.35	0.10		
4	P(28)	Yes	0.75	30	3	48	0.09	0.65	0.25	0.06	0.02	0.017
5	P(20)	Yes	1.0	30	3	48	0.10	0.70	0.30	0.07	0.02	
6	P(20)	No	0.25	2000	0.3	44	0.005	0.85	—	0.13	0.05	0.010
7	P(28)	Yes	0.25	30	0.3	29	0.06	0.70	0.13	0.01	0.03	0.003
8	P(14)	No	0.40	4500	0.7	60		0.75		0.10		

[a] Absorbed in the sample.

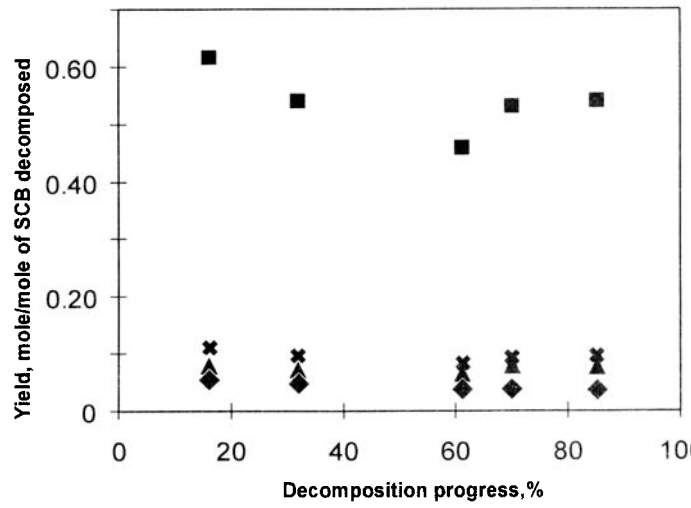

Figure 4 Product distribution in LPD of SCB: ■, C_2H_4; ×, $CH_3CH = CH_2$; ▲, CH_3SiH_3; ◆, CH_4.

The irradiation of these compounds in the presence of SF_6 occurs apparently through primary absorption by SF_6 (as a photosensitized process[27,28] since absorptivity (in $kPa^{-1}\,cm^{-1}$) at the wavelength of the irradiating P(20) line (944 cm^{-1}) of SF_6 (2.2) is much higher than that of SCB (0.0034 and DSCB (0.020).

Silacyclobutane

The IRMPD of SCB at pressures of 0.3–4.0 kPa was studied using the strongly absorbed irradiation lines P(14), P(20) and P(28) at 949.48, 944.19 and 936.80 cm^{-1}, respectively. The irradiation of SCB leads, regardless of the selected wavenumbers, to the formation of gaseous ethene (as a major product), propene, methane, methylsilane and n-propylsilane, and also to the deposition of a solid white material. With higher energy density (focused radiation), the decomposition rate is enhanced. The gaseous products also contain ethyne, while the deposited material shows a grey colour. The yields of gaseous products are given, and the enhancement of the decomposition by focused radiation is illustrated, in Table 1.

LPD of SCB, carried out with equimolar mixtures of SCB and SF_6 (each 0.8–2.4 kPa) in an excess of argon (34–38 kPa) resembles the IRMPD in products: ethene, as a major product, is accompanied by propene, methane and methylsilane. The mean effective temperature[49] of this decomposition can be estimated from similar irradition conditions reported previously[50,51] as ranging between 800 and 900 K. The absence of ethyne among the gaseous products can be ascribed to lower peak temperatures in LPD compared with IRMPD. A typical progress of LPD is illustrated in Fig. 4, which shows that the distribution of products is independent of the progress of decomposition, and that ethene is a major product throughout all the conversions.

The determined absolute amounts of gaseous products can be rationalized in terms of the previously reported[13,21–23] reactions (Scheme 3) and reveal that both IRMPD and LPD of SCB are dominated by ethene elimination (Route 1). The ratio C_2H_4/CH_3CHCH_2 being 6:1 for LPD, and even greater than that for IRMPD, indicates that in these decompositions elimination of propene is much less important than in the conventional low-pressure pyrolysis of SCB ($C_2H_4/CH_3CHCH_2 \cong 3 : 1$)[13], or in the surface decomposition of SCB.[16] It is tempting to ascribe this difference to the enhancement of Route 2 compared with Route 3, as being due to the elimination of effects of hot surfaces under our conditions. The very low yields of n-propyl- and methylsilane indicate the minor occurrence of reactions[52] of molecular hydrogen with the presumed silene and silylenes. In IRMPD, dihydrogen is apparently formed by secondary dehydrogenation, yielding ethyne. However, C_2H_2 not being observed in LPD, implies another route for H_2 formation, which can also be a direct dehydrogenation of SCB. This reaction, which is in fact a major route in the SCB surface decomposition (when H_2 and C_2H_4 eliminations operate in 2:1 ratio),[16] is ensued by the formation

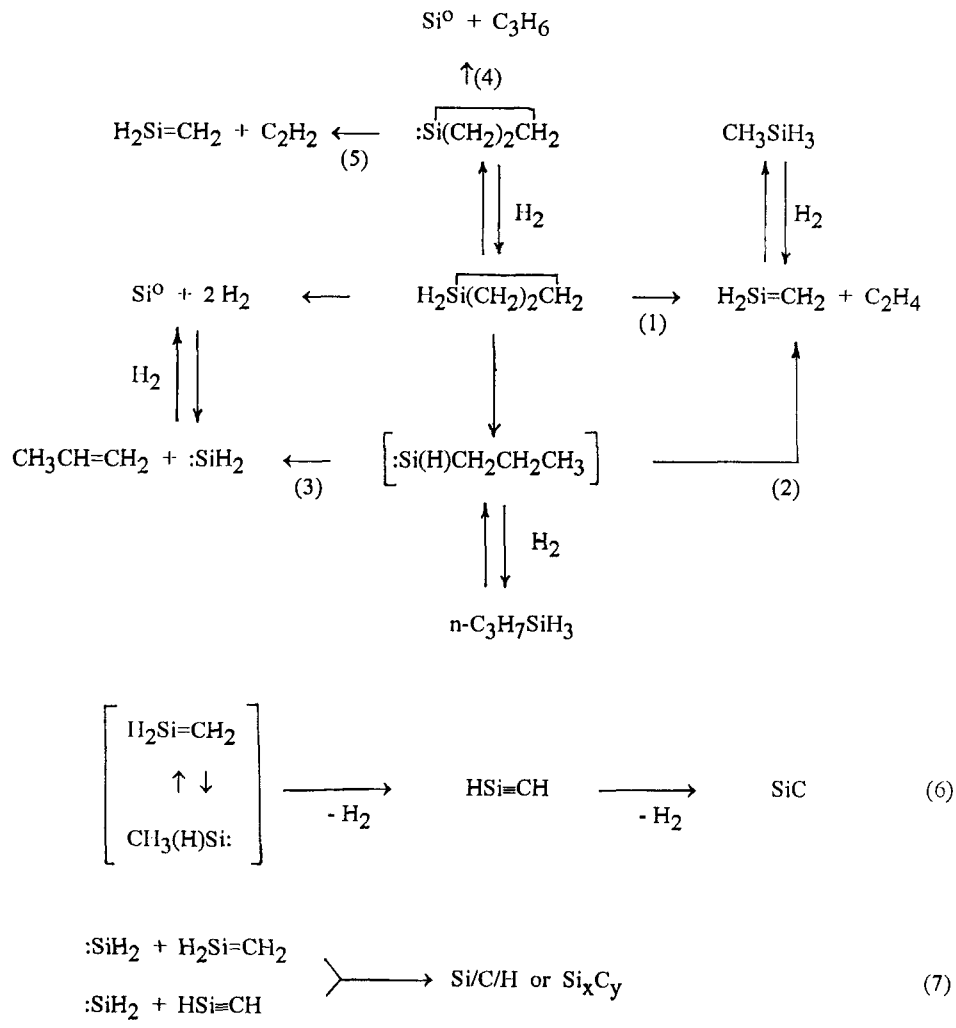

Scheme 3 Reactions involved in IRMPD and LPD of SCB.

of propene and elemental silicon (Route 4), or by the formation of silene and ethyne (Route 5). The latter seems less likely, but it would explain the absence of elemental silicon in the solid deposit. However, the high yields of ethene, and low but relatively significant yield of propene, make us believe that the major source of dihydrogen is dehydrogenation of silene (or its isomer methylsilylene) (Route 6). Properties of the solid deposit [the presence of SiC and not silicon (Si^0); see below] indicate that intermediary $H_2Si{=}CH_2$ [or $CH_3(H)Si$:] and/or products of their recombination (polymerization) can lose hydrogen and yield Si/C/H and SiC materials poorer in hydrogen than the $SiCH_4$ species. This dehydrogenation of $SiCH_4$ can be the result of an excess of energy in the irradiated system due to the exothermicity of the primary ethene elimination and also due to direct excitation of silene by the laser radiation. The absence of silicon (Si^0 in the solid deposit suggests the occurrence of reactions (Route 7) which 'scavenge' minor amounts of silylene and incorporate it into a Si/C framework.

In an attempt to detect silene (or methylsilylene) and silyne (or its more stable[34] isomer 1-silavinylidene) through addition of these species, IRMPD of SCB was carried out in an excess of buta-1,3-diene. However, these experiments yielded the same gaseous products and deposits as the runs without the trapping agent.

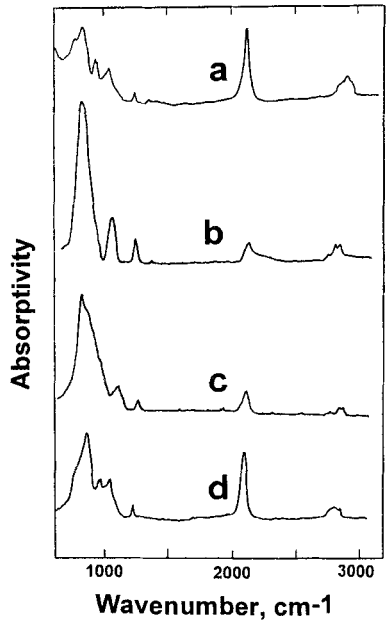

Figure 5 FTIR spectra of the deposit from SCB: **a**, run 1; **b**, run 4; **c**, run 5; **d**, LPD.

Representative FTIR spectra of the deposits produced by IRMPD and LPD of SCB are given in Fig. 5. The spectra show the typical pattern of SiC:H films and can be interpreted[53–55] as due to the vibrational modes compiled in Table 2.

The difference between our spectrum and the previously reported[37] IR spectrum of poly(silene), consisting of well-defined narrow absorption bands of almost equal absorptivity at 760, 851, 950 and 1046 cm^{-1}, prompts us to assume that the deposits **a–d** (Fig. 5) contain much less hydrogen than does poly(silene). The spectra of the deposits formed in IRMPD with nonfocused radiation (**a**) or in LPD (**d**) are dominated by strong absorption associated with ν(Si—C) and ν(Si—H) vibrations, while those of the deposits obtained in IRMPD with focused radiation (**b**, **c**) possess only one very strong band due to ν(Si—C). The $A_{\nu(Si—C)} : A_{\nu(Si—H)}$ ratio for these two cases is 0.71 (run 1) or 1.0 (LPD), and 4.7 (run 5) or 17.6 (run 4), respectively (Table 2). This difference implies that the latter deposits are still poorer in hydrogen than the former ones.

It is known[56] that more carbon incorporation in the Si–Si framework shifts the ν(Si—H) wavenumber to higher values and that a ν(Si—H) absorption above 2110 cm^{-1} corresponds to $a-Si_{1-x}C_x$: H films with carbon content $x>0.8$. Our data and the observation of $\nu(Si—H)>2130\ cm^{-1}$ confirm that the films resembling silicon carbide, formed when higher-energy fluxes are applied, have a very similar content of Si and C atoms.

The FTIR spectra are consistent (1) with the above presumed dehydrogenation of silene (or methylsilylene) during all laser-induced experiments, and (2) with a more pronounced dehydrogenation when the radiation is focused. The relative content of C—H and Si—H bonds in the deposits can be estimated[57] using the per-bond Si—H and C—H oscillator strengths in SiH_4 and CH_4 (or in $(CH_3)_nSiH_{4-n}$: n = 1, 2) compounds, even though such estimates deteriorate due to poor proportionality between this integrated strength and H concentration for different modes of sample preparation.[58] The ν(C—H) absorptivity being lower than that of ν(Si—H) by a factor of ~ 5 (Fig. 5, **a**, **c**, **d**) may indicate roughly equal distribution of H between Si and C, while comparable ν(C—H) and ν(Si—H) absorptivity in **b** implies that more hydrogen is bonded to C. Since both ν(C—H) and $\delta_s(CH_3Si)$

Table 2 FTIR spectra of the deposits from SCB

	Wavenumber (cm^1) Absorptivity[a]			
Vibrational mode	Run 1	Run 4	Run 5	LPD
ν(Si—C)[b]	820/0.71	808/17.6	825/4.7	831/1.0
Rock. and wag. CH_x	910/0.36	—	—	—
$\nu(SiCH_2Si)$	1025/0.32	1049/8.9	1070/0.9	1018/0.18
$\delta_s(CH_3Si)$	1250/0.10	1263/2.2	1265/0.18	1248/0.14
νSi—H)	2115/1.0	2135/1.0	2149/1.0	2951/1.0
ν(C—H)	2920/0.21	2932/1.2	2927/0.20	—
νC—H)	—	2964/1.3	2960/0.30	2951/0.15

[a] Normalized to absorptivity of ν(Si—H). [b] Also rock CH_3.

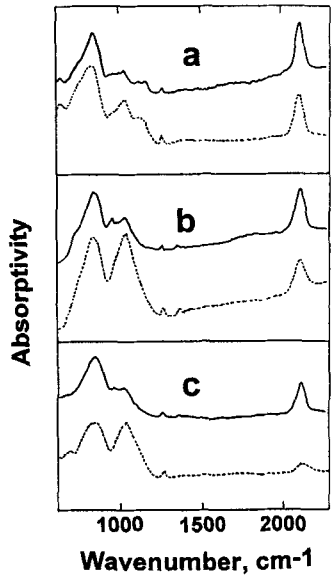

Figure 6 FTIR spectra of the solid materials from LPD of SCB (**a**), LPD of DSCB (**b**) and IRMPD of DSCB (**c**) as deposited (full line) and heated to 400 °C (broken line).

absorptivities are increased in **b**, this indicates that the increased H content in **b** is associated with more CH_3 groups, which in turn proves that silene→methylsilylene isomerization (preceding the polymerization) is more important with the focused irradiation employing the P(28) line.

The effect of annealing on the absorption bands between 700 and 2300 cm^{-1} is shown in Fig. 6. As the film is annealed at 400 °C, the ν(Si—C) and $\delta_S(CH_3Si)$ absorptivities do not change, while that of ν(Si—H) is decreased by almost 50%, and that of a band at 1035 cm^{-1} increases. The last band can be assigned to CH_n rocking/wagging modes and a Si–O stretch. We assume that the film loses hydrogen upon annealing and adsorbs oxygen when subsequently exposed to air.

The inferred process of dehydrogenation of silene (methylsilylene) and ensuing recombination/polymerization of $SiCH_n$ ($n<4$) species is supported from ESCA analyses of representative deposits (Table 3; Figs 7, 8). The stoichiometries found for the deposits reveal that the silicon- and carbon-containing materials incorporated oxygen; concentrations of Si, C and O do not significantly alter after ion sputtering of superficial layers, which indicates that the depositing Si/C/H materials are extremely sensitive to oxygen, which can penetrate to some depth in the superficial layers of the bulk material. This sensitivity can be accounted for by fast addition of molecular oxygen to the Si=C[59] (and perhaps some minor Si=Si[60]) bonds. We believe that the oxygen is present in superficial layers only and that the absorption band at 1020–1100 cm^{-1} is not contributed to by ν(Si—O) vibrations. (The ESCA analysis of superficial layers (~5 nm) was

Table 3 ESCA analysis of the deposits from SCB

Run	Stoichiometry	Core-level binding energies (eV)			Auger parameter, (eV)
		Si(2*p*)	C(1*s*)	O(1*s*)	
2	$Si_{1.0}C_{1.6}O_{0.8}$	102.0	248.8	532.7	1712.2
		102.2[a]	284.8[a]	532.8[a]	1712.3[a]
9[b]	$Si_{1.07}C_{1.6}O_0$	102.1	284.8	532.7	
			287.1		
5	$Si^{\alpha}_{0.75}Si^{\beta}_{0.25}C^{\alpha}_{0.77}C^{\beta}_{0.50}O_{0.6}$	100.1	282.5	531.8	1714.6
		102.2	284.8		1712.1
4	$Si^{\alpha}_{0.70}Si^{\beta}_{0.30}C^{\alpha}_{0.64}C^{\beta}_{0.38}C^{\gamma}_{0.1}O_{0.7}$	100.4	282.8	532.3	1714.8
		102.4	284.8		1711.9
			289.0		
10[c]	$Si_{1.0}C_{1.6}O_{0.48}$	102.0	248.8	532.7	1712.0[a]
			286.0		
11[d]	$Si_{1.0}C_{1.7}O_{0.82}$	102.2	284.8	532.8	1712.6
			287.6		

[a] Measured after ion sputtering (5 min, $E=4.5$ keV, $I=15$ μA (run 9); 4 min, $E=4$ keV, $I=40$ μA (run 10).

[b] 3 kPa, energy absorbed 1 J, nonfocused radiation, 2000 pulses, 66% conversion, P(20) line.

[c] 4 kPa, energy absorbed 0.6 J, nonfocused radiation, 1500 pulses P(14) line.

[d] LPD.

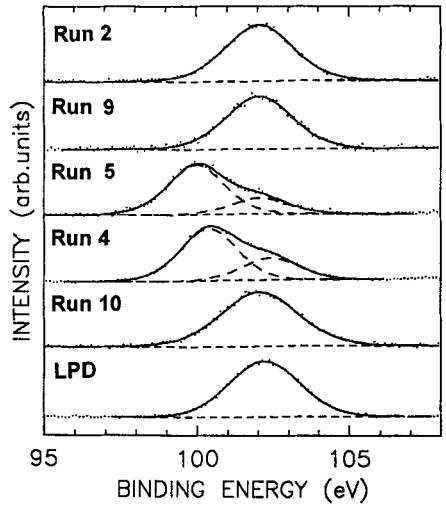

Figure 7 The Si(2*p*) core-level spectra of the deposits from SCB.

carried out after removing the deposits from the evacuated reactor and exposing them to air.) The core-level binding energies of the silicon and carbon and the shape of the Si(2*p*) and C(1*s*) spectral bands reveal the occurrence of chemically inequivalent forms, one being an organosilicon (oxygen-containing) Si/C/H polymer and the other one a silicon carbide. The relative SiC/polymer concentration is affected by irradiation conditions: thus the decomposition of the Si(2*p*) and C(1*s*) spectra of different deposits (Figs 7 and 8) reveals that, in accordance with the conclusions drawn from the FTIR spectra, the organosilicon polymer is mostly produced in runs 2 and 9, while the SiC materials predominate from runs 4 and 5. The above assignments of the spectral bands to particular chemical states of Si and C are based on comparison of the measured values of Si(2*p*) and C(1*s*) core-level binding energies, Si ($KL_{23}L_{23}$) kinetic energies and resulting values of the Auger parameters with the published data.[61,62]

Scanning electron microscopy analysis reveals that the deposits consist of agglomerates whose size ranges from less than 1 μm to more than 10 μm. Typically, the deposits containing SiC have a more discontinuous structure than those consisting of the organosilicon polymer (Fig. 9). This difference is obviously related to a greater tendency of the latter particles to polymerize in the deposition process.

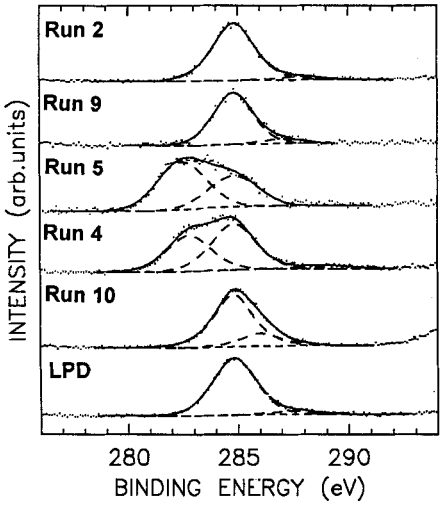

Figure 8 The C(1*s*) core-level spectra of the deposits from SCB.

Disilacyclobutane

IRMPD of DSCB (0.8–3.3 kPa) with the irradiating wavelengths at 974.62, 975.93 and 979.71 cm^{-1} results in the formation of minute amounts of gaseous methane, ethene, ethyne, propene, methylsilane and dimethylsilane (Table 4), and a high-yield deposition of a solid material. Of the hydrocarbons, methane is an important product and the total yield of methylsilane and dimethylsilane corresponds to 10% or less of the decomposed DSCB. This indicates that DSCB decomposes into a transient species, which then produces a solid deposit.

IRMPDs of DSCB carried out in the presence of buta-1,3-diene result in the formation of the same products as observed in the experiments without this trapping agent. The intermediacy of silene (and methylsilylene) is consistent with the detection of significant, although minor, amounts of their adduct with butadiene in the mass spectrum, (*m/z*, relative intensity): 98 (44), 97 (100), 96 (26), 83 (53), 81 (19), 71 (12), 70 (31), 55 (14), 53 (12), 43 (16)). Attempts to provide evidence for silyne (or 1-silavinylidene) through the detection of their adduct to two butadiene molecules were unsuccessful and are possibly related to very fast polymerization reactions yielding solid deposits.

LPD of DSCB carried out with equimolar amounts of DSCB and SF_6 (each 2.3 kPa) leads to the same products in similar distribution (in mol/mol of DSCB decomposed): CH_4 (0.032),

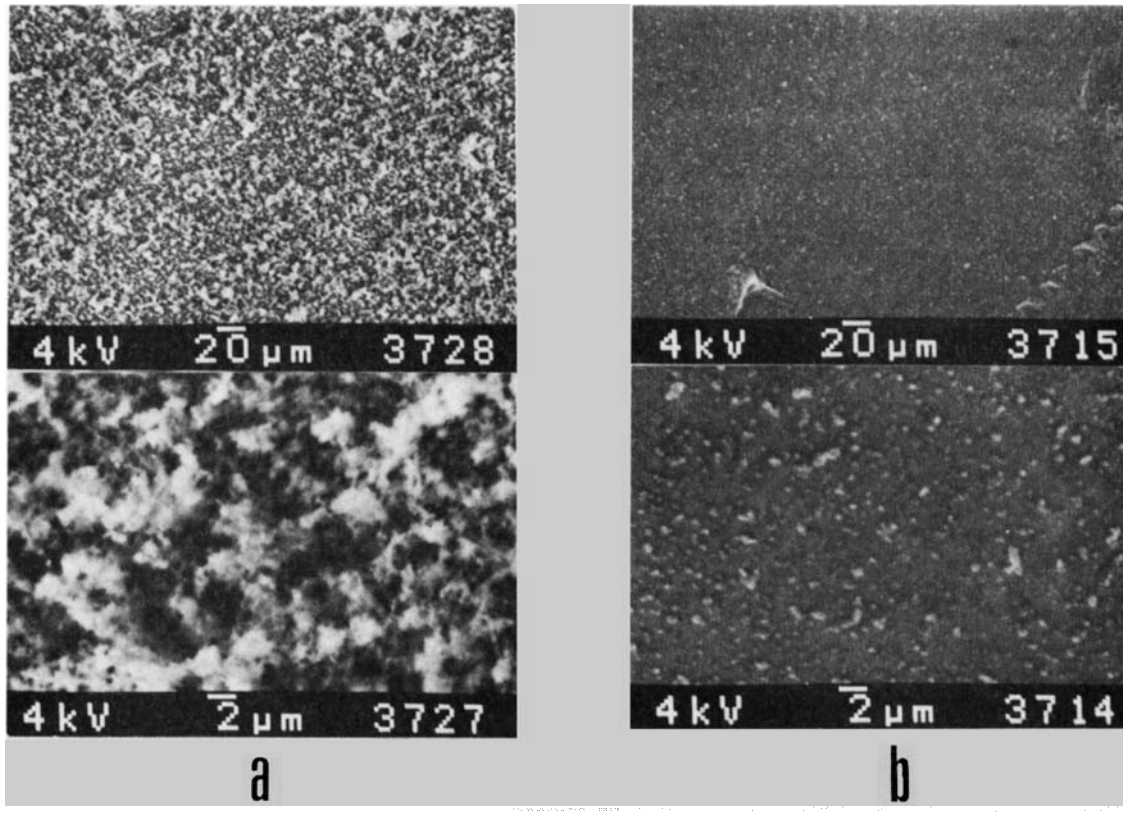

Figure 9 SEM images of the deposits from SCB: (a) run 3; (b) LPD.

C_2H_4 (0.044), $CH_3CH : CH_2$ (0.013), CH_3SiH_3 (0.10), and $(CH_3)_2SiH_2$ (0.14).

The observed yields of gaseous products are different from those found in conventional low-pressure pyrolysis, where CH_4, C_2H_4, CH_3SiH_3 and $(CH_3)_2SiH_2$ are formed in ratios 1:1:5:20.[26]

Methylsilane and dimethylsilane were deduced[26] to arise from a sequence of reactions consisting of DSCB homolytic cleavage and H-rearrangements producing the diradical $\cdot H_2SiCH_2SiH(CH_3)\cdot$ which is further cleaved and reacts with hydrogen (Scheme 4), or rearranges into $:Si(H)SiH(CH_3)_2$

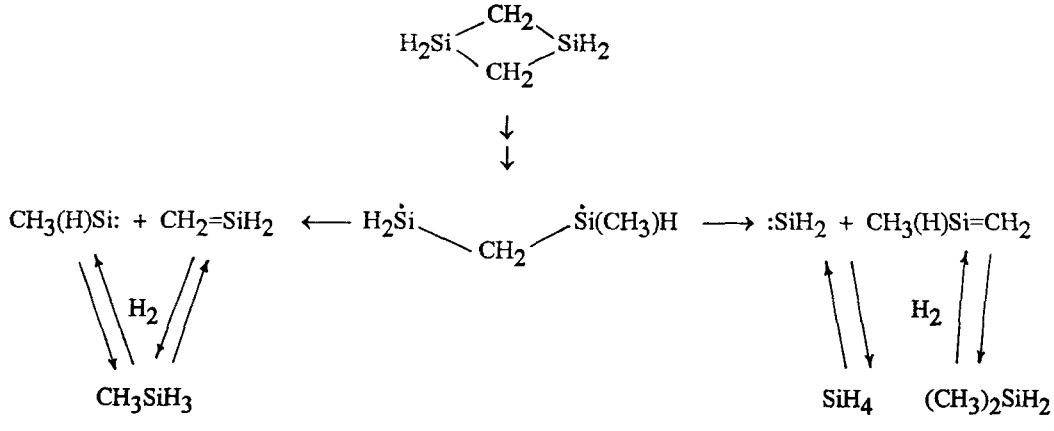

Scheme 4 Homolytic cleavage and subsequent reaction sequence in IRMPD or LPD of DSCB.[26]

Table 4 IRMPD of DSCB

Run	Irradn line	Focused	Energy in pulse[a] (J)	No. of pulses	Pressure (kPa)	Decompn. progress (%)	Gaseous products (mol/mol of DSCB decomposed)					
							CH_4	C_2H_4	C_2H_2	$CH_3CH : CH_2$	CH_3SiH_3	$(CH_3)_2SiH_2$
12	R(26)	No	1.0	2000	3.3	65	0.012	0.006	0.002	0.0001	0.051	0.082
13	R(20)	No	0.90	2000	3.3	74	0.015	0.007	0.002	0.0010	0.047	0.07
14	R(18)	No	1.0	300	2.7	62	0.01	0.01	0.03	0.020	0.028	—
15	R(20)	Yes	0.75	30	3.3	56	0.03	0.01	0.017	0.0001	0.01	0.011
16	R(26)	Yes	0.75	30	3.3	53	0.07	0.003	0.05	0.0003	0.03	0.028
17	R(18)	Yes	1.0	30	2.3	64	0.010	0.06	0.08	—	0.03	—
18	R(18)	No	1.0	100	0.8	50	0.027	0.08	0.04	0.01	0.10	—
19	R(26)	No	0.25	2000	0.3	62	0.009	0.01	0.003	—	0.08	0.08
20	R(26)	Yes	0.25	30	0.3	48	0.05	0.05	0.10	—	0.06	0.06

[a] Absorbed in the sample.

Table 5 FTIR spectra of the deposits from DSCB

Vibrational mode	Wavenumber (cm^{-1})/Absorptivity[a]				
	Run 12	Run 13	Run 16	Run 17	LPD
ν(Si—C)[b]	829/1.10	824/1.40	812/12.7	818/12.4	833/1.30
Rock. and Wag. CH_x	953/0.59	950/0.63	—	—	950/0.30
$\nu(SiCH_2Si)$	1030/0.40	997/0.24	1058/0.70	1047/1.2	1020/0.45
		1030/0.18	1105/0.70		
$\delta_s(CH_3Si)$	1248/0.10	1248/0.16	1263/0.70	1261/0.40	1250/0.10
$\delta_{as}(CH_3Si)$	1352/0.09	1350/0.05	—	—	1361/0.08
ν(Si—H)	2114/1.0	2110/1.0	2154/1.0	2137/1.0	2112/1.0
ν(C—H)	2885/0.05	2923/0.11	—	2926/0.5	2923/0.09
ν(C—H)	2955/0.03	2952/0.08	2964/0.20	—	2951/0.08

[a] Normalized to absorptivity of ν(Si—H). [b] Also rock. CH_3.

which inserts into DSCB and produces a trisilane which further enters into a variety of decomposition routes. While these reactions apparently occur also in the irradiated systems, small quantities of both silanes produced during both IRMPD and LPD reveal that the extent of reaction of silene and methylsilylene with dihydrogen is strongly decreased at the expense of $SiCH_4$ dehydrogenation and ensuing polymerization. The occurrence of these dominating reactions, being proved by FTIR and ESCA analysis of the deposits (see below), reveals that the main decomposition routes of DSCB are those described in Scheme 1 and 2. Similarly to SCB, IRMPD of DSCB also yields, depending on the irradiation flux (0.25–5.6 J cm^{-2}, focused or nonfocused radiation), polymeric Si/C/H or SiC deposits.

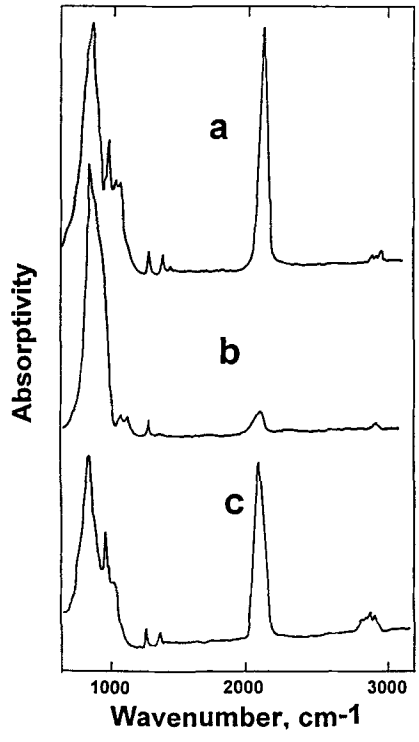

Figure 10 FTIR spectra of the deposit from DSCB: **a**, run 12; **b**, run 16 or 20; **c**, LPD.

Representative FTIR spectra (Table 5; Fig. 10) show that (1) the deposits contain less hydrogen that polysilene;[37] (2) the deposits found in IRMPD with nonfocused radiation or in LPD possess two very strong bands of almost equal absorptivity associated with ν(Si—C) and ν(Si—H); and (3) the deposits from IRMPD with focused radiation have only one very strong band in the ν(Si—C) region.

The $A_{\nu(Si—C)}:A_{\nu(Si—H)}$ ratios for these two different experimental conditions being 1.1–1.4:1 and more than 12:1, respectively, indicate that $SiCH_4$ dehydrogenation is enhanced when the radiation is focused. The content of Si—H and C—H bonds (determined from relative absorptivities at ν(Si—C) and ν(Si—H)) resembles that in the deposits from SCB. Higher absorptivities for ν(Si—H) and $\delta_S(CH_3Si)$, e.g. in runs 16 and 17, indicate that the increased H content is brought about by more CH_3 groups, which in turn proves that the silene→methylsilylene rearrangement is in these cases more important than in others. The ν(Si—H) absorption for the SiC-like films formed with higher-energy fluences is observed at >2130 cm^{-1}. This indicates, as in similar deposits from SCB, that the films have roughly an equal content of Si and C atoms.

The effect of annealing on the IR spectra is

Table 6 ESCA analysis of the deposits from DSCB

Run	Stoichiometry	Core-level binding energies (eV)			Auger parameter, (eV)
		Si(2*p*)	C(1*s*)	O(1*s*)	
12	$Si_{1.00}C_{1.4}O_{0.7}$	102.1	284.8	532.9	1712.3
	$Si_{1.00}C_{1.0}O^{a}_{1.0}$	102.2[a]	284.8	533.4	1714.3
13	$Si_{1.00}C_{1.8}O_{0.9}$	101.9	284.8	532.7	1712.1
	$Si_{1.00}C_{1.2}O^{a}_{0.7}$	102.2[a]	284.8[a]	532.8[a]	1714.5[a]
14	$Si_{1.00}C_{1.01}O_{0.43}$	101.7	284.8	533.0	
15	$Si^{\alpha}_{0.86}Si^{\beta}_{0.15}C^{\alpha}_{0.68}C^{\beta}_{0.33}C^{\gamma}_{0.21}O_{0.5}$	100.9	283.1		1714.2
		102.8	284.9	532.6	1711.1
			286.4		
16	$Si^{\alpha}_{0.85}Si^{\beta}_{0.14}C^{\alpha}_{0.62}C^{\beta}_{0.34}C^{\gamma}_{0.07}O_{0.4}$	100.8	283.1	532.5	1714.2
		102.7	284.8		1711.1
			286.2		
19	$Si_{1.00}C_{1.8}O_{1.0}$	102.2	284.8	532.6	1711.7
20	$Si^{\alpha}_{0.77}Si^{\beta}_{0.25}C^{\alpha}_{0.64}C^{\beta}_{0.55}O_{0.7}$	100.6	282.9	532.1	1714.5
		102.3	284.8		1712.1
LPD	$Si_{1.00}C_{1.30}O_{0.82}$	102.1	284.8	532.3	1712.9
	$Si_{1.00}C_{1.05}O_{0.69}$ [a]	102.4	284.9	533.4	1712.8

[a] Measured after ion sputtering (5 min, $E=4.5$ keV, $I=15$ μA).

demonstrated in Fig. 6. When the temperature of the substrate is increased to 400 °C, a decrease of ν(Si—H) absorptivity by about 55% and a significant increase of the absorptivity at 1035 cm^{-1} is found. In analogy to the deposit from SCB, these changes reflect incorporation of oxygen into the Si–C framework due to the reactivity of naked silicon atoms or Si=C (and Si=Si) bonds[59,60] towards oxygen.

The implications on dehydrogenation (rearrangement) of silene, which precedes the polymerization of $SiCH_n$ ($n<4$), and apparently of HSi≡CH and SiC, species, are supported by ESCA analyses (Table 6; Figs 11 and 12) of representative deposits.

Similarly to the deposits from SCB, those from DSCB also contain oxygen which cannot be removed by ion sputtering, and may therefore be incorporated in some depth of superficial layers. The binding energies and shapes of the silicon and

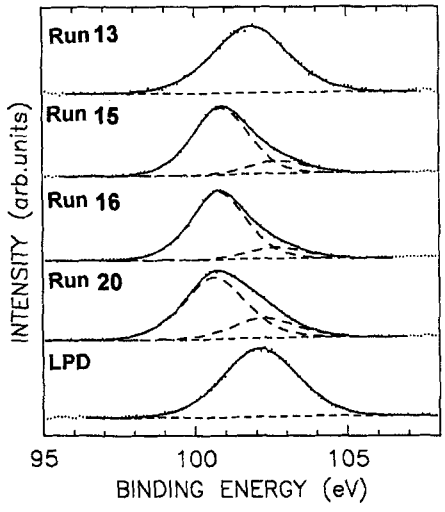

Figure 11 The Si(2*p*) core-level spectra of the deposits from DSCB.

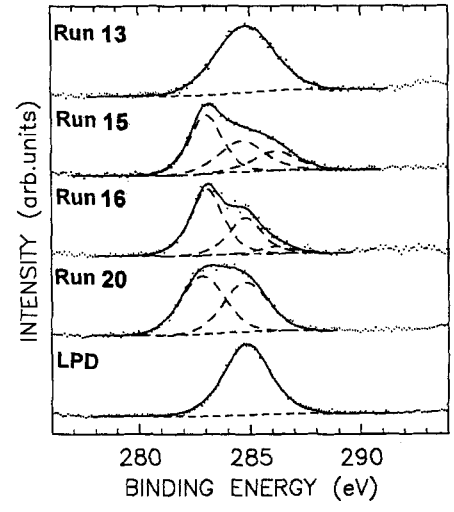

Figure 12 The C(1s) core-level spectra of the deposits from DSCB.

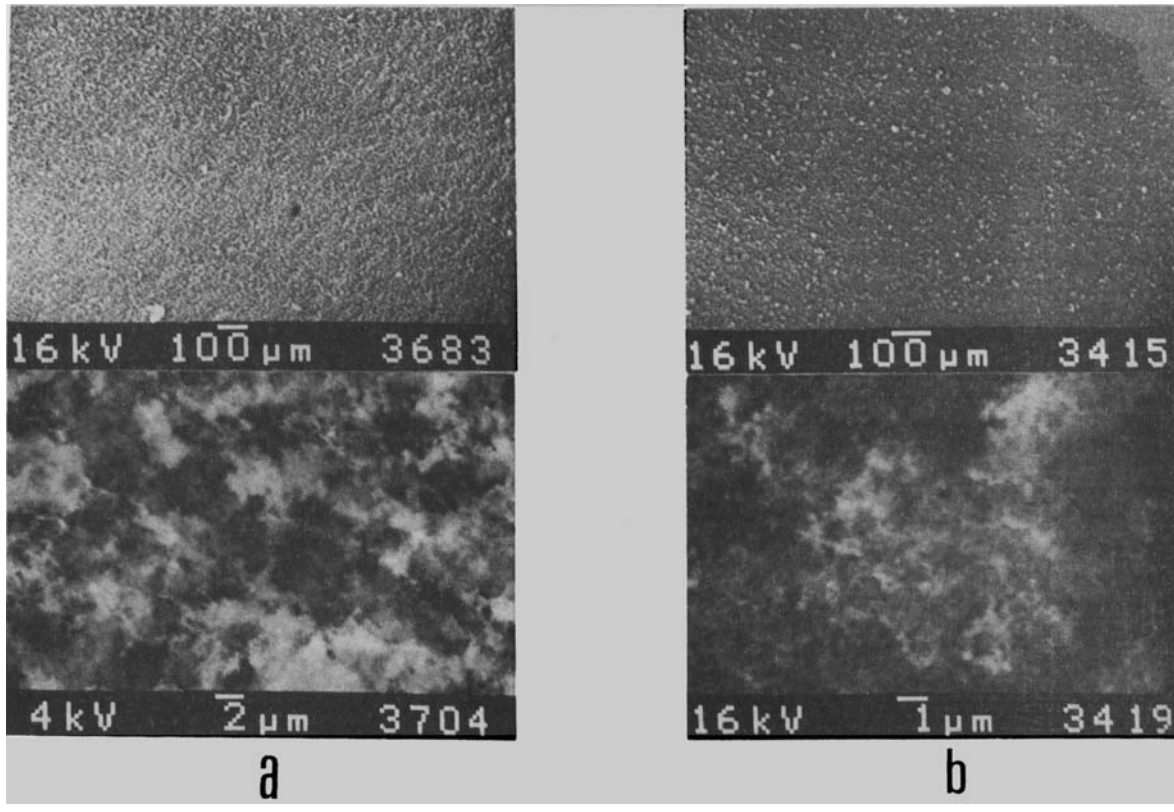

Figure 13 SEM images of the deposits from DSCB: (a) run 15; (b) run 14.

carbon photoemission lines reveal the presence of two different forms of these elements, one incorporated in the (oxygen-containing) organosilicon Si/C/H polymer, and the other present in SiC. The SiC/polymer ratio depends on the irradiating conditions: the curve fitting of the Si(2*p*) and C(1*s*) spectra of several deposits shows, in accordance with the FTIR spectra, that the organosilicon polymer is preferred in LPD and IRMPD with nonfocused radiation (run 13), while mostly SiC is formed when IRMPD with focused radiation is performed (runs 15, 16, 20).

SEM images show that the deposits have fluffy structures, which do not differ whether they were obtained using focused and nonfocused radiation, or by LPD (Fig. 13).

CONCLUSIONS

In summary, the laser-induced decomposition of SCB and DSCB is a clean reaction producing silene (and methylsilylene). These transients very efficiently polymerize, or dehydrogenate and polymerize, to yield copious amounts of Si/C/H and SiC particles. The films produced are sensitive towards ambient oxygen. The IRMPD of both silacycles appears promising for low-temperature chemical vapour deposition of silicon carbide.

Acknowledgement The authors greatly appreciate the financial assistance of the Volkswagen Stiftung. H.B. thanks the Deutsche Forschungsgemeinschaft for financial support. The support of the Grant Agency of the Czech Republic (grant no. 203-93-0204) is also gratefully acknowledged.

REFERENCES

1. W. Böcker and H. Hausner, *Ber. Dt. Keram. Ges.* 233 (1978).
2. Y. Okabe, J. Hojo and A. Kato, *J. Less-Com. Met.* **68**, 29 (1979).
3. M. Endo, T. Sano, K. Mori, N. Urasato and M. Shiraishi, *Yogyo Kyakaishi* **95**, 104 (1987).

4. J. A. O'Neil, M. Horsburg, J. Tann, K. J. Grant and G. L. Paul, *J. Am. Ceram. Soc.* **72**, 1130 (1989).
5. A. E. Kaloyeras, J. W. Corbett, P. J. Toscano and R. B. Rizk, *Mater. Res. Soc. Symp. Proc.* **192**, 601 (1990).
6. V. A. Zubov, M. Friedrich, H. D. Klotz, R. Fricke, M. Wesche and H. Prost, *Zh. Neorg. Khim.* **35**, 2917 (1990).
7. D. E. Cagliostro and S. R. Riccitiello, *J. Am. Ceram. Soc.* **73**, 607 (1990).
8. H. Schmidbaur, R. Hager and J. Zech, in: *Frontiers of Organosilicon Chemistry*, Bassindale, A. R. and Gaspar, P. P. (eds), The Royal Society of Chemistry, Cambridge, 1991, p. 62.
9. Y. M. Li and B. F. Fieselmann, *Appl. Phys. Lett.* **59**, 1720 (1991).
10. A. Figueras, S. Garelik, J. Santiso, R. Rodriguez-Clemente, B. Armas and C. Combescure, *Mater. Sci. Eng. B* 1183 (1992).
11. E. F. Hengge, in: *Abstracts of Lectures, Xth Int. Symp. on Organosilicon Chemistry*, Poznan, Poland, 1993, p. 42.
12. I. M. T. Davidson, in: *Silicon Chemistry*, Corey, E. R., Corey, J. Y. and Gaspar, P. P. (eds), Horwood, Chichester, 1988, p. 269.
13. I. M. T. Davidson, A. Fenton, S. Ijadi-Maghsoodi, R. J. Scampton, N. Auner, J. Grobe, N. Tillman and T. J. Barton, *Organometallics* **3**, 1593 (1984).
14. G. Maier, G. Mihm, H. P. Reisenauer and D. Littmann, *Chem. Ber.* **117**, 2369 (1984).
15. B. A. Sawrey, H. E. O'Neal, M. A. Ring and D. Coffey, *Int. J. Chem. Kinet.* **16**, 7 (1984); **16**, 23 (1984); **16**, 31 (1984).
16. A. D. Johnson, J. Perrin, J. A. Mucha and D. E. Ibbotson, *J. Phys. Chem.* **97**, 12937 (1993).
17. O. P. Strausz, K. Obi and W. K. Duholke, *J. Am. Chem. Soc.* **90**, 1359 (1968).
18. K. Obi, A. Clement, H. E. Gunning and O. P. Strausz, *J. Am. Chem. Soc.* **91**, 1622 (1969).
19. M. A. Ring, H. E. O'Neal, S. F. Rickborn and B. A. Sawrey, *Organometallics* **2**, 1891 (1983).
20. P. S. Neudorfl, E. M. Lown, I. Safarik, A. Jodhan and O. P. Strausz, *J. Am. Chem. Soc.* **109**, 5780 (1987) and refs therein.
21. A. K. Maltsev, V. N. Khabasheku and O. M. Nefedov, *Dokl. Akad. Nauk SSSR* **247**, 383 (1979).
22. C. M. Golino, R. D. Bush and L. H. Sommer, *J. Am. Chem. Soc.* **97**, 7371 (1975).
23. R. T. Conlin and R. S. Gill, *J. Am. Chem. Soc.* **105**, 618 (1983).
24. G. Maier, G. Mihm and H. P. Reisenauer, *Chem. Ber.* **117**, 2351 (1984).
25. G. Maier, G. Mihm and H. P. Reisenauer, *Angew. Chem., Int. Ed. Engl.* **20**, 597 (1981).
26. N. Auner, I. M. T. Davidson, S. Ijadi-Maghsoodi and F. T. Lawrence, *Organometallics* **5**, 431 (1986), and refs therein.
27. D. K. Russell, *Chem. Soc. Rev.* **19**, 407 (1990).
28. J. Pola, *Spectrochim. Acta, Part A* **46**, 607 (1990).
29. J. Pola, in: *Lasers in Atomic, Molecular and Nuclear Physics*, Letokhov, V. S. (ed.), World Scientific, Singapore, 1987, p. 166.
30. J. Pola, V. Chvalovský, E. A. Volnina and L. E. Gusel'nikov, *J. Organomet. Chem.* **341**, C13 (1988).
31. J. Pola, E. A. Volnina and L. E. Gusel'nikov, *J. Organomet. Chem.* **391**, 275 (1990).
32. D. Čukanová and J. Pola, *J. Organomet. Chem.* **453**, 17 (1993).
33. L. E. Gusel'nikov and N. S. Nametkin, *Chem. Rev.* **79**, 529 (1979).
34. G. Raabe and J. Michl, *Chem. Rev.* **85**, 419 (1985).
35. Z.-F. Zhang, F. Babonneau, R. M. Laine, Y. Mu, J. F. Harrod and J. A. Rahn, *J. Am. Ceram. Soc.* **74**, 670 (1991).
36. T. Kobayashi, T. Sakakura, T. Hayashi, M. Yumura and M. Tanaka, *Chem. Lett.* 1157 (1992).
37. H.-J. Wu and L. V. Interrante, *Polym. Prepr. (Am. Chem. Soc., Div. Polym. Chem.)* 32 (1991).
38. T. L. Smith, US patent 4 631 179, 23 Dec. 1986.
39. L. V. Interrante, C. K. Whitmarsh, T. K. Trout and W. R. Schmidt, in: *Inorganic and Organometallic Polymers with Special Properties*, Laine, R. M. (ed.), Kluwer Academic, Amsterdam, 1992, p. 243.
40. D. J. Larkin and L. V. Interrante, *Chem. Mater.* **4**, 22 (1992).
41. G. Guelachvili and K. Navahari Rao, *Handbook of Infrared Standards*, Academic Press, SDan Diego, 1986.
42. J. Pola, M. Farkacová, P. Kubát and A. Trka, *J. Chem. Soc., Faraday Trans. 1* **80**, 1499 (1984).
43. J. H. Scofield, *J. Electron Spectrosc. Relat. Phenom.* **8**, 129 (1976).
44. M. P. Seah and W. A. Dench, *Surface Interface Anal.* **1**, 1 (1979).
45. A. E. Hughes and B. A. Sexton, *J. Electron Spectrosc. Relat. Phenom.* **48**, 31 (1988).
46. J. Laane, *J. Am. Chem. Soc.* **89**, 1144 (1967).
47. N. S. Nametkin, V. M. Vdovin, L. E. Gusel'nikov and V. I. Zav'yalov, *Izv. Akad. Nauk SSSR, Ser. Khim.* 584 (1966).
48. R. M. Irwin, J. M. Cooke and J. Laane, *J. Am. Chem. Soc.* **99**, 3273 (1977).
49. W. M. Shaub and S. H. Bauer, *Int. J. Chem. Kinet.* **7**, 509 (1975).
50. P. Kubát and J. Pola, *Coll. Czech. Chem. Commun.* **50**, 1548 (1985).
51. P. Kubát and J. Pola, *Z. Phys. Chem. (Leipzig)* **268**, 849 (1987).
52. I. Safarik, V. Sandhu, E. M. Lown, O. P. Strausz and T. N. Bell, *Res. Chem. Int.* **14**, 105 (1990).
53. S. Ray, D. Das and A. K. Barna, *Solar Energ. Mat.* **15**, 45 (1987).
54. H. Rübel, B. Schröder, W. Fuhs, J. Krauskopf, T. Rupp and K. Bethge, *Phys. Stat. Sol.* **139**, 131 (1987), and refs therein.
55. H. Bürger, *Organomet. Chem. Rev. A* **3**, 425 (1968).
56. D. M. Bhusari and S. T. Kshirsagar, *Mater. Lett.* **11**, 348 (1991).
57. H. C. Low and P. John, *J. Organomet. Chem.* **201**, 363 (1980), and refs therein.
58. H. Shanks, C. J. Fung, L. Ley, M. Cardona, F. J. Demond and S. Kalbitzer, *Phys. Stat. Sol.* **100**, 43 (1980).
59. I. M. T. Davidson, C. E. Dean and F. T. Lawrence, *J. Chem. Soc., Chem. Commun.* 52 (1981).

60. R. West, H. B. Yokelson, G. R. Gillette and A. J. Millevolte, in: *Silicon Chemistry*, Corey, E. R., Corey, J. Y. and Gaspar, P. P. (eds), Horwood, Chichester, 1988, p. 269.
61. C. D. Wagner, *NIST X-ray Photoelectron Spectroscopy Database*, NIST Std. Ref. Database 20, US Dept. of Commerce, Gaithersburg, 1991.
62. D. Briggs and M. P. Seah, *Practical Surface Analysis by Auger and X-ray Photoelectron Spectroscopy*, Wiley, Chichester, 1983, p. 488.